Fiber-optic confocal microscopy using a spatial light modulator

Pierre M. Lane, Andrew L. P. Dlugan, Rebecca Richards-Kortum,* and Calum E. MacAulay

Cancer Imaging Department, British Columbia Cancer Research Center, 601 West 10th Avenue, Vancouver, British Columbia V5Z 1L3, Canada

Received August 1, 2000

We present a novel fiber-optic confocal microscope in which the scanning operation is achieved by use of a spatial light modulator (SLM) to sequentially illuminate individual fibers or patterns of multiple fibers. Experimental images are presented, and the optical-sectioning capability of the device is demonstrated. The novel SLM-based system is more optically efficient, achieves higher contrast, and has improved optical-sectioning capabilities compared with those of other proposed instruments for confocal microendoscopy.

OCIS codes: 180.0180, 170.1790, 170.2150, 230.6120.

Several research groups have proposed extensions of the confocal microscope to permit *in vivo* imaging. These extensions generally involve the miniaturization and relocation of the objective lens (and in some cases the beam-scanning optics) to the distal end of an optical fiber so that the fiber assembly can be inserted through a hypodermic needle, a catheter, or the biopsy channel of an endoscope. In general, two different approaches in the literature can be identified. The first involves a single optical fiber and the relocation of both the $x-y$ scanning function and the objective lens to the distal end of the fiber.[1–3] The second approach employs a coherent bundle of several thousand fibers and retains the scanning function at the proximal end of the bundle.[4,5]

Various techniques have been proposed to provide mechanical $x-y$ scanning at the distal end of an optical fiber. Such scanning can be achieved in principle by translation of either the optical fiber[1] or the objective lens.[2] One group demonstrated a scanning confocal microscope based on micromachined scanning mirrors.[3] In their device a single-mode optical fiber illuminates two silicon torsional scanning mirrors with orthogonal axes of rotation.

Devices in which only the objective lens and the z-axis scan are relocated to the distal end of the fiber employ a coherent bundle of several thousand optical fibers. In these systems the proximal end of a coherent imaging bundle is placed in the object plane of a commercial confocal microscope. Gmitro and Aziz demonstrated confocal imaging by use of a confocal laser-scanning microscope,[4] and Juskaitis *et al.* employed a tandem scanning microscope.[5] In both cases, an illumination spot (or set of spots) scanned over the proximal face of the imaging bundle is transferred to the distal end and consequently imaged into the specimen by a second lens system.

Several researchers have observed decreased contrast and poor optical-sectioning ability when a spot is scanned over the face of a fiber bundle in the conventional manner.[6,7] As a conventional spot moves over the bundle, it illuminates not only the core material of each fiber but also its cladding and the interfiber material. Consequently, at any given time, one or more fibers, and the inactive material between those fibers, are illuminated. Photons from a single scanning spot that are coupled into more than one fiber degrade the optical-sectioning ability of the microscope. Photons that are incident upon the inactive region between fiber cores may be backscattered (owing to Fresnel reflections from the face of the bundle and autofluorescence from the interfiber material) and decrease system contrast. Photons that are not backscattered are randomly coupled into a nearby fiber (possibly several fibers away from the desired fiber) and further decrease the system's optical-sectioning ability. In addition, the illumination spot spends a significant amount of time illuminating multiple fibers, fiber cladding, and the inactive space between fibers. This time results in wasted illumination energy and lost data-acquisition time.

The solution proposed in this Letter is to employ a spatial light modulator (SLM) to discretely translate a single spot (or pattern of spots) across the fiber bundle. The SLM and the imaging bundle are arranged to be in conjugate image planes so that there is a one-to-many mapping of fibers to SLM pixels. The active region of an arbitrary fiber in the bundle can be illuminated, without illuminating the inactive space between fibers, by turning on the appropriate group of SLM pixels. A set of fibers can be illuminated in parallel by simultaneous activation of those pixels associated with each of the fibers in the set. A SLM is naturally suited to this scanning problem because it is straightforward to accurately register specific SLM pixels with each active fiber core in the bundle. It would be very difficult to achieve this goal with a conventional mechanical or acousto-optic scanning system.

The system illustrated in Fig. 1 was constructed to demonstrate confocal imaging through a fiber bundle. A digital micromirror device (DMD) from Texas Instruments (Dallas, Tex.) was employed as the SLM because of its high contrast, high pixel count, and fast temporal response. The DMD micromirrors have a center-to-center spacing of 17 μm and a mechanical switching time of 15 μs.[8] A 640 $\times$ 480 resolution DMD with a full on–off contrast ratio of 255:1 was employed in this work; devices with higher resolution (1280 $\times$ 1024) and increased contrast (370:1) are now available. DMD's have been used by several

0146-9592/00/241780-03$15.00/0

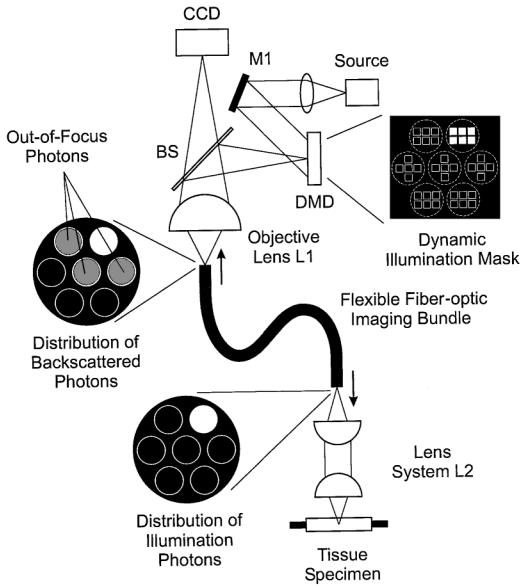

Fig. 1. Experimental setup. Individual fiber cores within the imaging bundle are illuminated by activation of an appropriate set of DMD mirrors. M1, plane mirror; BS, beam splitter.

groups[9–11] for confocal imaging but have not been employed, to our knowledge, in a confocal microendoscopy system.

As shown in Fig. 1, a Sumitomo IGN-08/30 image guide [30,000 fibers, 2-μm fiber diameter, 3-μm center-to-center spacing, 0.35 numerical aperture (NA)] was positioned in the object plane of a conventional microscope configured for reflected-light illumination. The DMD was positioned in the illumination path of the microscope so that it was conjugate to the object plane. The contrast of the DMD is maximized because the image-side NA of a microscope objective is generally much less than the maximum value of 0.18 suggested by Hornbeck[8] for optimum contrast. A CCD camera was positioned in the primary image plane of the microscope. The DMD was uniformly illuminated with blue (400–500-nm) filtered light from an EFOS (Mississauga, Ontario, Canada) X-Cite mercury arc lamp. The objective lens, L1, was a Nikon 20× Plan Apochromat.

The DMD mirrors and CCD pixels were registered with the fibers of the image bundle in a two-step calibration procedure. First, a plane mirror was positioned in the object plane of the microscope (the proximal end of the image bundle as shown in Fig. 1 was temporarily replaced with a plane mirror). A registration pattern was written to the DMD, and an image was acquired with the CCD camera. This first registration image was used to map DMD mirrors to CCD pixels. The image bundle was then placed in the object plane of the microscope and illuminated at its distal end. An image of the fiber bundle was acquired. This second registration image was used to map fibers in the bundle to CCD pixels. Together, the two registration images were employed to map DMD mirrors to individual fibers. In the experimental results reported here, there were, on average, six mirrors mapped to each fiber in the bundle. The mapping of mirrors to fibers for seven typical fibers is illustrated in the illumination mask of Fig. 1.

A fiber in the image bundle was illuminated by activation of those mirrors on the DMD that correspond to that fiber. At the distal end of the fiber, photons from an illuminated fiber were relayed into the specimen by lens system L2. This double-objective lens system was composed of two Nikon Plan Achromat lenses (20× 0.75-NA and 60× 1.40-NA oil immersion) placed back to back around a field lens to provide 3× magnification. In-focus structures located within the specimen at the object plane backscattered photons to the illuminating fiber. Out-of-focus structures, above or below the object plane, backscattered photons to the set of fibers surrounding the illuminating fiber. The system constructed a confocal image by saving the in-focus photons (those that were backscattered into the same fiber from which they were launched) and discarding the out-of-focus photons.

The optical efficiency of the illumination path was determined by measurement of the optical power that was incident upon the proximal end of the fiber bundle and that emitted from its distal end. When only those mirrors assigned to individual fiber cores were activated, the optical efficiency was 30%. This efficiency includes losses that were due to fiber attenuation, Fresnel reflections at each end of the fiber bundle, and any fiber–mirror misalignment. When the entire fiber bundle was illuminated by activation of all the mirrors, the optical efficiency dropped to 19%. The efficiency dropped under full illumination because light that was incident upon the inactive material between fiber cores is not efficiently transmitted by the fiber bundle. This wasted light is either backscattered, reducing the contrast of the system, or coupled into the cladding and then either absorbed by the fiber jacket or recoupled into a nearby fiber.

Images acquired with the experimental system are illustrated in Fig. 2. Figures 2(a)–2(c) show conventional (wide-field) images of an Intel 80486 microprocessor imaged at three different focal planes. The corresponding confocal images are shown in Figs. 2(d)–2(f). The axial distance between the focus levels is 2 μm, and the scale bar on each image is

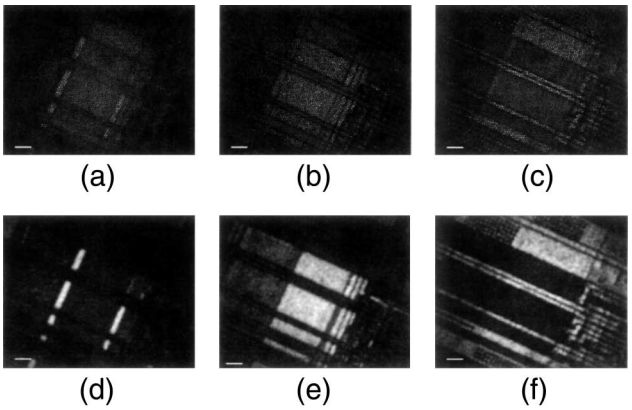

Fig. 2. Images of a Intel 486 microprocessor: (a)–(c) wide-field images at three different focal planes, (d)–(f) confocal images at the same levels. The scale bars are 10 μm.

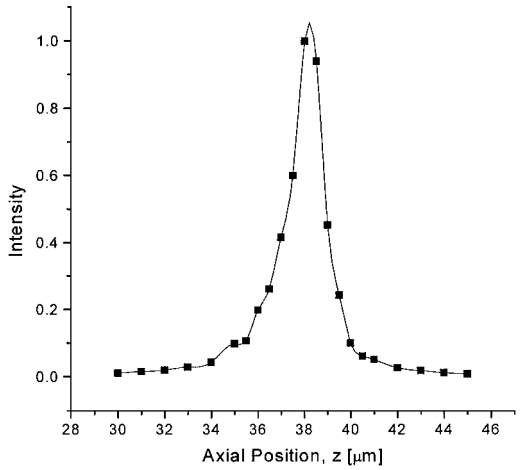

Fig. 3. Axial response of a plane mirror scanned through the focus. The FWHM is 1.6 μm.

10 μm long. The optical-sectioning capability of the system is clearly evident from a comparison of the wide-field and the confocal images. In-focus features appear in both sets of images; out-of-focus features appear in only the wide-field images and are absent from the confocal images. The fiber structure is clearly visible in the three wide-field images. In the confocal case the fiber structure is not as visible because the total in-focus intensity integrated over the core area of each fiber was written to the final image as a smooth Gaussian spot. An average gray level of 25 was observed at the fiber cores when the signal reflected from the target was blocked. The in-focus structures that caused the fibers to just saturate the 8-bit detector therefore had a contrast of 10:1. Much higher contrasts are anticipated when the fiber bundle is properly coupled to the objective lenses by use of an index-matching fluid.

The axial response of the system was characterized by translation of a plane mirror through focus. The response when a single fiber at the center of the field was illuminated is shown in Fig. 3. The FWHM is 1.6 μm. In this confocal system each fiber in the imaging bundle serves the function of an illumination and detection pinhole. The effective diameter of the confocal pinhole is therefore determined by the average diameter of the fibers. The normalized diameter of the pinhole, projected through lens system L2 into object space, is $\nu_p = kd_0\ \mathrm{NA}/M$, where $k = 2\pi/\lambda$, d_0 is the fiber diameter, and M is the magnification. Here we assume that the diameter of the fiber core is equal to the FWHM of its intensity distribution, $d_0 \approx d_{\mathrm{FWHM}} = 2.5\ \mu$m. The NA of lens system L2 is $3 \times 0.35 = 1.05$ (the effective NA of the lens system is limited by the NA of the imaging bundle projected through the lens). At a wavelength of $\lambda =$ 450 nm, $\nu_p = 6.11$, and consequently the theoretical variation of on-axis intensity with defocus is not described well by the simple sinc(z) paraxial formula. Following the method of Wilson and Carlini,[12] we calculated a theoretical FWHM of 1.07 μm for this confocal system. The difference in the theoretical and the observed FWHM's is due mainly to the nonuniform photon density across the fiber pinhole. The theoretical calculation assumes uniform illumination and detection pinhole functions, which is clearly not true for a fiber illumination pinhole with a Gaussian-like intensity distribution.

By employing a SLM to selectively illuminate individual fibers rather than simply scanning a spot over the fiber bundle, we can dramatically improve the optical-sectioning ability of a fiber-optic confocal microscope. In a conventional scanned-spot system, as the spot passes over the interfiber region of the fiber bundle, as many as three fibers can be illuminated simultaneously (assuming hexagonal fiber packing). Because the spot intensity is redistributed as the light propagates down each of the three fibers, the effective pinhole diameter is increased by at least a factor of 2. The increase in pinhole diameter dramatically reduces the optical-sectioning capability of the system, particularly when the normalized pinhole diameter is greater than 2. When fibers are illuminated individually by a SLM, only one fiber is illuminated at a time, and the effective pinhole diameter is always equal to the diameter of the fiber. This leads to a smaller FWHM and enhanced optical sectioning. In addition, illuminating individual fibers with a SLM leads to higher contrast and improved optical efficiency, because all photons that are incident upon the fiber bundle are coupled into a specific fiber core, and very few photons are backscattered from the interstitial material between fibers.

P. M. Lane's e-mail address is plane@bccancer.bc.ca.
*Also with the Biomedical Engineering Program, Department of Electrical and Computer Engineering, University of Texas, Austin, Texas 78731.

References

1. T. Dabbs and M. Glass, Appl. Opt. **31,** 3030 (1992).
2. L. Giniunas, R. Juskatis, and S. V. Shatalin, Electron. Lett. **27,** 724 (1991).
3. D. L. Dickensheets and G. S. Kino, Opt. Lett. **21,** 764 (1996).
4. A. F. Gmitro and D. Aziz, Opt. Lett. **18,** 565 (1993).
5. R. Juskaitis, T. Wilson, and T. F. Watson, Proc. SPIE **2655,** 92 (1996).
6. Y. S. Sabharwal, A. R. Rouse, L. Donaldson, M. F. Hopkins, and A. F. Gmitro, Appl. Opt. **38,** 7133 (1999).
7. R. Juskaitis, T. Wilson, and T. F. Watson, Scanning **19,** 15 (1997).
8. L. J. Hornbeck, Proc. SPIE **3013,** 27 (1997).
9. M. Liang, R. L. Stehr, and A. W. Krause, Opt. Lett. **22,** 751 (1997).
10. P. J. Verveer, Q. S. Hanley, P. W. Verbeek, L. J. Van Viliet, and T. M. Jovin, J. Microsc. (Oxford) **189,** 192 (1998).
11. C. E. MacAulay and A. Dlugan, Proc. SPIE **3260,** 201 (1998).
12. T. Wilson and A. R. Carlini, Opt. Lett. **12,** 227 (1987).